

# Targeting Noncanonical Pyroptosis With a Small Molecular Inhibitor Alleviates Inflammation in the LPS-Induced Keratitis Mouse Model

Yun Zhang,<sup>1-3</sup> Nenghua Zhou,<sup>4</sup> Yan Jiao,<sup>5</sup> Guifeng Lin,<sup>2</sup> Xun Li,<sup>1,3</sup> Sheng Gao,<sup>1,3</sup> Pei Zhou,<sup>4</sup> Jingming Liu,<sup>2</sup> Jinshan Nan,<sup>2</sup> Meixia Zhang,<sup>1,3</sup> and Shengyong Yang<sup>2</sup>

<sup>1</sup>Department of Ophthalmology, West China Hospital, Sichuan University, Chengdu, China

<sup>2</sup>State Key Laboratory of Biotherapy and Cancer Center, West China Hospital, Sichuan University, Chengdu, China

<sup>3</sup>Research Laboratory of Macular Disease, West China Hospital, Sichuan University, Chengdu, China

<sup>4</sup>Key Laboratory of Drug Targeting and Drug Delivery System of Ministry of Education, West China School of Pharmacy, Sichuan University, China

<sup>5</sup>Laboratory of Anesthesia and Critical Care Medicine, Department of Anesthesiology, Translational Neuroscience Center, West China Hospital, Sichuan University, Chengdu, China

Correspondence: Meixia Zhang, Department of Ophthalmology, West China Hospital, Sichuan University, Chengdu 610041, China;

[zhangmeixia@scu.edu.cn](mailto:zhangmeixia@scu.edu.cn)

Shengyong Yang, State Key Laboratory of Biotherapy and Cancer Center, West China Hospital, Sichuan University, Chengdu 610041, China; [yangsy@scu.edu.cn](mailto:yangsy@scu.edu.cn)

YZ and NZ are equal contribution to this work.

**Received:** September 28, 2022

**Accepted:** December 13, 2022

**Published:** January 3, 2023

Citation: Zhang Y, Zhou N, Jiao Y, et al. Targeting noncanonical pyroptosis with a small molecular inhibitor alleviates inflammation in the LPS-induced keratitis mouse model. *Invest Ophthalmol Vis Sci*. 2023;64(1):1.

<https://doi.org/10.1167/iovs.64.1.1>

**PURPOSE.** Pyroptosis, a novel proinflammatory programmed cell death, has been implicated in some ocular diseases. Of special note is the noncanonical pyroptosis that has recently been recognized to play a critical role in microbial keratitis. We previously discovered a new potent small molecular pyroptosis inhibitor, J114. In this investigation, we will explore whether J114 is able to inhibit the noncanonical pyroptosis and the underlying mechanism. Then a lipopolysaccharide (LPS)-induced keratitis mouse model will be used to evaluate the therapeutic effect of J114 in vivo.

**METHODS.** In vitro, macrophages originating from humans or mice were stimulated with intracellular LPS to induce noncanonical pyroptosis activation. In vivo, acute keratitis in mouse was induced by LPS intrastromal injection. We verified the protective effect of J114 on noncanonical pyroptosis. Clinical scoring, histological observation, macrophage localization, and quantification of pyroptotic markers in the cornea were used to characterize the therapeutic effects.

**RESULTS.** J114 substantially inhibited the noncanonical pyroptosis and the release of inflammatory cytokines by suppressing the activation of caspase-4/5/11 and the noncanonical NLRP3 inflammasome through blocking the NLRP3-ASC interaction. In vivo, J114 protected against LPS-induced noncanonical pyroptosis of acute keratitis, as manifested by alleviated clinical manifestations and histological disorders, and relieved inflammatory reactions.

**CONCLUSIONS.** In this study, we found that J114 could efficiently inhibit LPS-induced noncanonical pyroptosis and revealed the underlying mechanism. This compound displayed significant anti-inflammatory activity in the LPS-induced keratitis mouse model. All the findings indicated that J114 could be a potential lead compound for drug development against inflammatory ocular surface diseases.

**Keywords:** noncanonical pyroptosis, acute keratitis, pyroptosis inhibitor, caspase-4/5/11, NLRP3 inflammasome

Inflammatory corneal disease can lead to corneal opacity, scarring, and even perforation, and cause serious damage to visual functions. Environmental irritants, allergens, and pathogens directly affect the ocular surface to cause lasting and recurrent destructive inflammatory damage, which would not stop immediately even when microbes were eliminated.<sup>1</sup> In the acute inflammatory process, lipopolysaccharide (LPS), also called endotoxin, one of the main components of the gram-negative bacilli cell wall, can be released from pathogens and identified by the innate immune system, subsequently producing extensive inflammatory factors to cause cell injury and cell death.<sup>2</sup> Except for antibiotics, anti-

inflammatory agents are needed to alleviate the immune response caused by the release of LPS. However, these drugs have relatively few options and some side effects.<sup>3</sup> Identifying and developing new drugs that both target well and achieve the desired efficiency is a challenging and urgent task.

The innate immune system maintains a delicate balance between inflammation and immune defense. Pyroptosis, an important part of the body's innate immune response, plays an indispensable role in antagonizing pathogen infection and sensing endogenous danger signals.<sup>4</sup> Various inflammasomes are assembled and activated in corneal inflam-

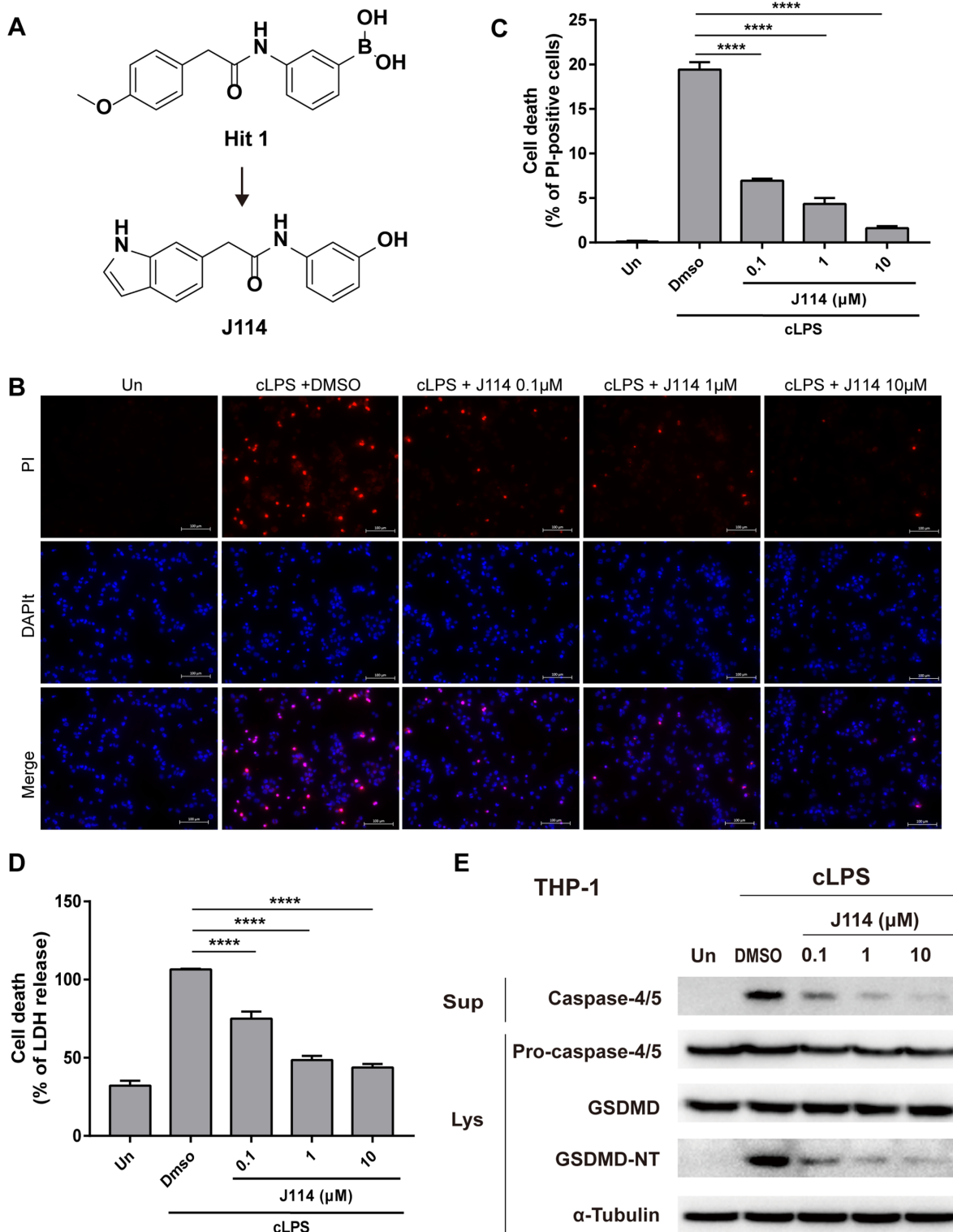


**FIGURE 1.** J114 inhibits caspase-4/5 activation and pyroptotic cell death in THP-1 macrophages. Cells were treated with the indicated doses of J114 for 30 minutes followed by transfection with 1 μg/mL lipopolysaccharide (LPS) overnight. **(A)** Structures of hit compound 1 and J114. J114 is a potent pyroptosis inhibitor after structural optimization from hit compound 1. **(B)** Lytic cell death was measured through staining with propidium iodide (PI, red) for 15 minutes and DAPI (5 minutes, blue). The image shows PI-positive cells merged with DAPI fluorescence. Scale bars, 100 μm. The result was representative of three independent experiments. **(C)** The percentage of PI-positive cells was the ratio of PI-positive to all cells (revealed by DAPI), which was calculated by counting six randomly chosen fields using ImageJ software. **(D)** Lytic cell death was assessed by the release of lactic acid dehydrogenase (LDH) into culture supernatants. Data are shown as the mean ± SEM (*n* = 3). **(E)** The supernatants (Sup) and lysates (Lys) were collected and analyzed by Western blotting to assess the indicated protein levels. The result was representative images of three independent experiments.

mation in response to bacterial, viral, fungal, and parasitic infections.<sup>5</sup> Of special note is the noncanonical pyroptosis that has recently been recognized to play a critical role in microbial keratitis.<sup>6,7</sup> The noncanonical cell pyroptotic death process is induced by intracellular LPS and then activates caspase-4/5/11, which in turn induces ATP release and K<sup>+</sup> efflux and activates the NLRP3 inflammasome to release activated IL-1 $\beta$ . Meanwhile, activated caspase-4/5/11 cleaves gasdermin D (GSDMD) to form pores on the cell membrane and cause pyroptosis.<sup>8,9</sup> This process still needs further exploration in inflammatory corneal disease.

Since the central role of inflammasomes in the pathogenesis of inflammation has been recognized, several small molecular pyroptosis inhibitors have been reported. However, numerous inhibitors exhibited unsatisfactory activity and no drugs have been approved thus far.<sup>10</sup> Our previous study designed and synthesized a potent pyroptosis inhibitor J114, *N*-(3-hydroxyphenyl)-2-(1*H*-indol-6-yl)acetamide, originating from structure optimization of hit 1 (Fig. 1A), which inhibited NLRP3-dependent activation of caspase-1 and the release of IL-1 $\beta$  more efficiently.<sup>11</sup> However, whether J114 can inhibit noncanonical pyroptosis and attenuate corneal inflammation is unclear. The therapeutic potential of J114 in the inflammatory injury of keratitis should be explored.

This study aims to explore the underlying mechanisms by which J114 inhibits noncanonical pyroptosis and to investigate the protective effect of J114 on LPS-induced keratitis mouse model *in vivo*. Our study may provide a potent therapeutic agent targeting noncanonical pyroptosis in inflammatory ocular surface diseases.

## METHODS

### Animals

C57BL/6 mice (7-8 weeks old, male mice) were purchased from Chengdu GemBio Co. (Chengdu, Sichuan, China). The mice were maintained in standard animal care conditions with free access to food and water. All animal experiments were performed under the approval of the Experimental Animal Management Committee of Sichuan University and conducted in accordance with the ARVO Statement for the Use of Animals in Ophthalmic and Vision Research.

### Reagents and Antibodies

LPS (O55:B5) (L4524), PMA (P1585), and propidium iodide (PI, #P4170) were purchased from Sigma-Aldrich. Lipofectamine 2000 (11668019) and Pam3CysSerLys4 (Pam3CSK4, #tlrl-pms) were purchased from InvivoGen (San Diego, CA, USA). A CytoTox 96 nonradioactive cytotoxicity assay kit (#G1781) was obtained from Promega (Madison, WI, USA). All the antibodies used in this study are listed in Supplementary Table S1.

### Cells

THP-1 cells, THP-1 ASC-KO cells (thp-koascz; Invitrogen) and THP-1 ASC-GFP reporter cells (thp-ascgfp; Invitrogen) were cultured in RPMI 1640 medium supplemented with 10% fetal bovine serum (FBS) and 1% penicillin/streptomycin. For THP-1-derived macrophages, THP-1 cells were differentiated with 300 nM PMA for 24 hours.

J774A.1 and RAW 264.7 cells were cultured in DMEM supplemented with 10% FBS and 1% penicillin/streptomycin at 37°C in a humidified incubator with 5% CO<sub>2</sub>.

### Inflammasome Stimulation

For noncanonical NLRP3 inflammasome activation, THP-1 ( $1 \times 10^6$  cells/mL) or J774A.1 ( $5 \times 10^5$  cells/mL) cells were plated in 6-well plates overnight. Cells were transfected with 1  $\mu$ g/mL LPS (for THP-1 cells) or 2.5  $\mu$ g/mL LPS (for THP-1 ASC-KO cells) overnight using Lipofectamine 2000 (Invitrogen) in Opti-MEM. Cells were primed with 1  $\mu$ g/mL Pam3CSK4 in DMEM for 4 hours and then transfected with 1  $\mu$ g/mL LPS (for J774A.1 cells) or 2.5  $\mu$ g/mL LPS (for RAW 264.7 cells) overnight using Lipofectamine 2000 (Invitrogen) in Opti-MEM. Before LPS transfection, cells were treated with DMSO or J114 for 30 minutes earlier.

### Cell Death Assay

Lytic cell death was measured by PI incorporation or lactic acid dehydrogenase (LDH) release. Cells were treated with DMSO or J114 for 30 minutes and then transfected with 1  $\mu$ g/mL LPS overnight using Lipofectamine 2000. J774A.1 cells were primed with 1  $\mu$ g/mL Pam3CSK4 for 4 hours earlier. PI (2  $\mu$ g/mL) solution together with DAPI was used to measure the percentage of lytic cell death. The cells were visualized under a fluorescence microscope (Zeiss). LDH release was measured using a CytoTox96 Non-Radioactive Cytotoxicity Kit (Promega) according to the manufacturer's instructions.

### Western Blot Analysis

After stimulation and J114 treatment as indicated, supernatants were collected for the preparation of soluble protein from the cell culture medium. Supernatants were centrifuged at 13,000 revolutions per minute (rpm) for 15 minutes at 4°C to remove cellular debris. Organic solvents (chloroform-methanol) were used to extract protein from the supernatants. The protein in cell lysates was extracted, separated by 12% SDS-PAGE and transferred to PVDF membranes. The membrane was blocked and incubated with the indicated primary antibody at 4°C overnight, followed by incubation with the appropriate HRP-conjugated secondary antibody for 1 hour at 37°C. The membranes were washed with TBST and subsequently imaged using a Super Lumia ECL HRP substrate kit (Abbkine).

### ELISA

The concentration of IL-1 $\beta$  in the cell culture supernatants was measured using ELISA kits (NeoBioscience and Proteintech) according to the manufacturer's instructions.

### ASC-Speck Formation

THP-1 ASC-GFP reporter cells were seeded at  $1 \times 10^6$ /mL on coverslips and treated with J114 for 30 minutes subsequently with LPS transfection. After that, the cells were fixed with 4% paraformaldehyde, and nuclei were stained with DAPI for 5 minutes. J774A.1 cells were seeded at  $3 \times 10^5$ /mL on coverslips. After Pam3CSK4 priming and LPS stimulation with J114, as previously described, the cells were fixed with 4% paraformaldehyde and permeabilized with 0.5% Triton

X-100. After blocking, the cells were incubated with the anti-mouse ASC antibody (#67824) overnight, followed by incubation with Cy3-conjugated AffiniPure goat anti-mouse IgG (SA00009-1) for 30 minutes. Nuclei were stained with DAPI for 5 minutes. The cells were visualized under a fluorescence microscope (Zeiss, Axio Imager M2).

### ASC Oligomerization

THP-1 and J774A.1 cells were transfected with LPS and treated with J114, as previously described. The cells were scraped in 1 mL ice-cold PBS containing 2 mM EDTA and centrifuged for 5 minutes at 1500 g at 4°C. Cell pellets were resuspended in 500  $\mu$ L of ice-cold buffer A (20 mM HEPES-KOH, pH 7.5, 10 mM KCl, 1.5 mM MgCl<sub>2</sub>, 1 mM EDTA, 1 mM EGTA, and 320 mM sucrose), lysed by shearing 30 times through a 21-gauge needle and centrifuged for 8 minutes at 300 g at 4°C. Transfer supernatants to new 1.5 mL Eppendorf tubes and remain 40  $\mu$ L supernatants as input controls. The supernatants were diluted with 1 volume of CHAPS buffer (20 mM HEPES-KOH, pH 7.5, 5 mM MgCl<sub>2</sub>, 0.5 mM EGTA, 0.1 mM PMSF, and 0.1% CHAPS) and centrifuged for 5 minutes at 2400 g at 4°C to pellet ASC oligomers. The supernatants were discarded, and the pellets were resuspended in 30  $\mu$ L of CHAPS buffer containing 2 mM DSS and then incubated for 20 minutes at 37°C to cross-link the proteins. After centrifugation for 8 minutes at 5000 g at 4°C, the supernatants were discarded, and the pellets were resuspended in 30  $\mu$ L of 2  $\times$  protein loading buffer. The samples were boiled for 10 minutes at 100°C.

### Intracellular ATP Measurement

The concentration of intracellular adenosine 5'-triphosphate (ATP) was detected using an Enhanced ATP Assay Kit (S0027, Beyotime) according to the manufacturer's instructions.

### Intracellular K<sup>+</sup> Measurement

The concentration of intracellular potassium was detected using the Potassium (K<sup>+</sup>) Turbidimetric Assay Kit (E-BC-K279-M, Elabscience) according to the manufacturer's instructions.

### Co-Immunofluorescence

Cells were treated as previously described. After fixing and permeabilizing, the cells were incubated with the anti-human ASC antibody (#13833) and anti-NLRP3 antibody (AG-20B-0014) overnight, followed by incubation with Cy3-conjugated AffiniPure goat anti-rabbit IgG (SA00009-2) and coralite 488-conjugated goat anti-mouse IgG (SA00013-1) for 30 minutes. Nuclei were stained with DAPI for 5 minutes. The cells were visualized under a confocal fluorescence microscope (Zeiss, LSM880).

### LPS-Induced Keratitis

C57BL/6 mice were intrastromal injected with 3  $\mu$ L of 1 mg/mL LPS as the keratitis group and saline for control mice after systemic anesthesia with sodium pentobarbital and topical anesthesia with one drop of oxybuprocaine hydrochloride. J114 (5 mg/mL, dissolved with F188) or F188 control (all diluted in saline) was topically deliv-

ered four times a day. Each group contained a minimum of 12 mice. Mouse corneas were collected 24 hours or 48 hours later for clinical scoring, hematoxylin and eosin (H&E) staining, flow cytometry, immunofluorescence staining, immunohistochemical (IHC) staining, ELISA, and Western blotting.

For clinical scoring, 0 to 5 days after modeling, the inflammatory response was confirmed and recorded with a slit lamp. A 4-point system was used based on a published protocol.<sup>12</sup> Briefly, 0 = normal, clear cornea; 1 = mild corneal haze, but still able to see iris structures; 2 = moderate corneal haze, difficult to see iris structures; 3 = significant corneal opacity, unable to see iris structures; and 4 = damage and loss of corneal tissue (including melt).

For Western blotting, mouse corneas were lysed in RIPA buffer (with 1% cocktail and 1 mM PMSF) on ice for 1 hour. The lysate was mixed with loading buffer and detected by Western blotting.

For H&E and IHC staining, the eyeball samples were fixed with improved fixative solution (paraformaldehyde and acetic acid), paraffin-embedded, dewaxed, rehydrated, and cut into 5- $\mu$ m sections. After slicing, H&E was stained conventionally, and IL-1 $\beta$  (AF-401-NA), caspase-1 (AF-401-NA), caspase-11 (sc-374615), NLRP3 (AG-20B-0014), CD11b (GB11058), and F4/80 (GB113373) were stained by immunohistochemistry. All images were acquired with Panoramic MIDI.

For safety assessment, J114 (5 mg/mL, dissolved with F188) or F188 control (all diluted in saline) was topically delivered 4 times a day continuously for 7 days. Clinical scoring, fluorescein staining and H&E staining were used to assess corneal epithelium injury.

For macrophage localization with flow cytometry, the corneas were dissected out (4 corneas per group) and digested with RPMI containing collagenase D (5 mg/mL) and DNase I (14 U/mL) in a 37°C bath for 1 hour with inverting every 10 minutes. Then, cell suspension was filtered through a 100  $\mu$ m strainer. The cells were washed with PBS containing 1% FBS and stained with CD45-FITC (103107, BioLegend), CD11b-APC (101211, BioLegend), F4/80-APC-Cy7 (123151, BioLegend), and CD86-PE-Cy7 (105013, BioLegend) antibodies for 30 minutes at room temperature. Subsequently, the cells were washed and resuspended with PBS. Finally, the cells were analyzed using NovoCyte Flow Cytometer (Agilent Technologies).

For double immunofluorescence staining, cryosections of the mouse eyeball specimens were blocked using 5% BSA and incubated with anti-CD11b (GB11058), anti-F4/80 (GB113373) and anti-IL-1 $\beta$  (AF-401-NA) overnight at 4°C. Followed by incubation with FITC-conjugated Affinipure goat anti-rabbit IgG and Cy3-conjugated Affinipure donkey anti-goat IgG. Nuclei were stained with DAPI. The tissues were visualized under a fluorescence microscope (Zeiss, Axio Imager M2).

### Statistical Analyses

All experiments were performed at least three times. Data are expressed as the mean  $\pm$  SEM and analyzed for statistical significance using unpaired, two-tailed Student's *t*-test (GraphPad Prism Software). Any *P* value < 0.05 was considered statistically significant. For all significant differences, \**P* < 0.05, \*\**P* < 0.01, \*\*\**P* < 0.001, and \*\*\*\**P* < 0.0001, ns: not significant.



## RESULTS

### J114 Inhibits the Activation of Caspase-4/5/11 and Pyroptosis In Vitro

We initially transfected LPS into the cytosol of THP-1 macrophage cells to stimulate noncanonical NLRP3 inflammasome activation. Indeed, PI staining and LDH release showed a lytic form of cell death after LPS transfection. J114 significantly protected the maintenance of membrane integrity and reduced the levels of LDH in the supernatants (Figs. 1B–D). Immunoblot analysis revealed that LPS transfection markedly increased the secretion of cleaved caspase-4/5 in the supernatant and the expression of the N-terminal fragment of GSDMD, indicating the activation of caspase-4/5 and the cleavage of GSDMD. Interestingly, active cleaved caspase-4/5 in supernatants was dose-dependently reduced by J114. Subsequent cleavage of GSDMD by active caspase-4/5 was also inhibited in a dose-dependent manner (Fig. 1E). Intracellular LPS can activate caspase-11 to initiate

noncanonical NLRP3 inflammasome activation in murine cells.<sup>13</sup> We next sought to verify these results in mouse J774A.1 macrophage cells. Due to the characteristic of species differences in J114 between human and mouse cells,<sup>11</sup> we raised the concentration of J114, which is still within a safe concentration range, through the analysis of cytotoxicity (Supplementary Fig. S1). The results showed that J114 also dose-dependently inhibited intracellular LPS-induced caspase-11 activation, GSDMD cleavage and pyroptotic cell death (Figs. 2A–C). Collectively, these results suggested that J114 potentially inhibited caspase-4/5/11 activation and noncanonical pyroptotic cell death in vitro.

### J114 Inhibits Noncanonical NLRP3 Inflammasome Activation In Vitro

Intracellular LPS-induced caspase-4/5 or caspase-11 activation can mediate noncanonical NLRP3 inflammasome pathway activation, which relies on ATP release and K<sup>+</sup> efflux

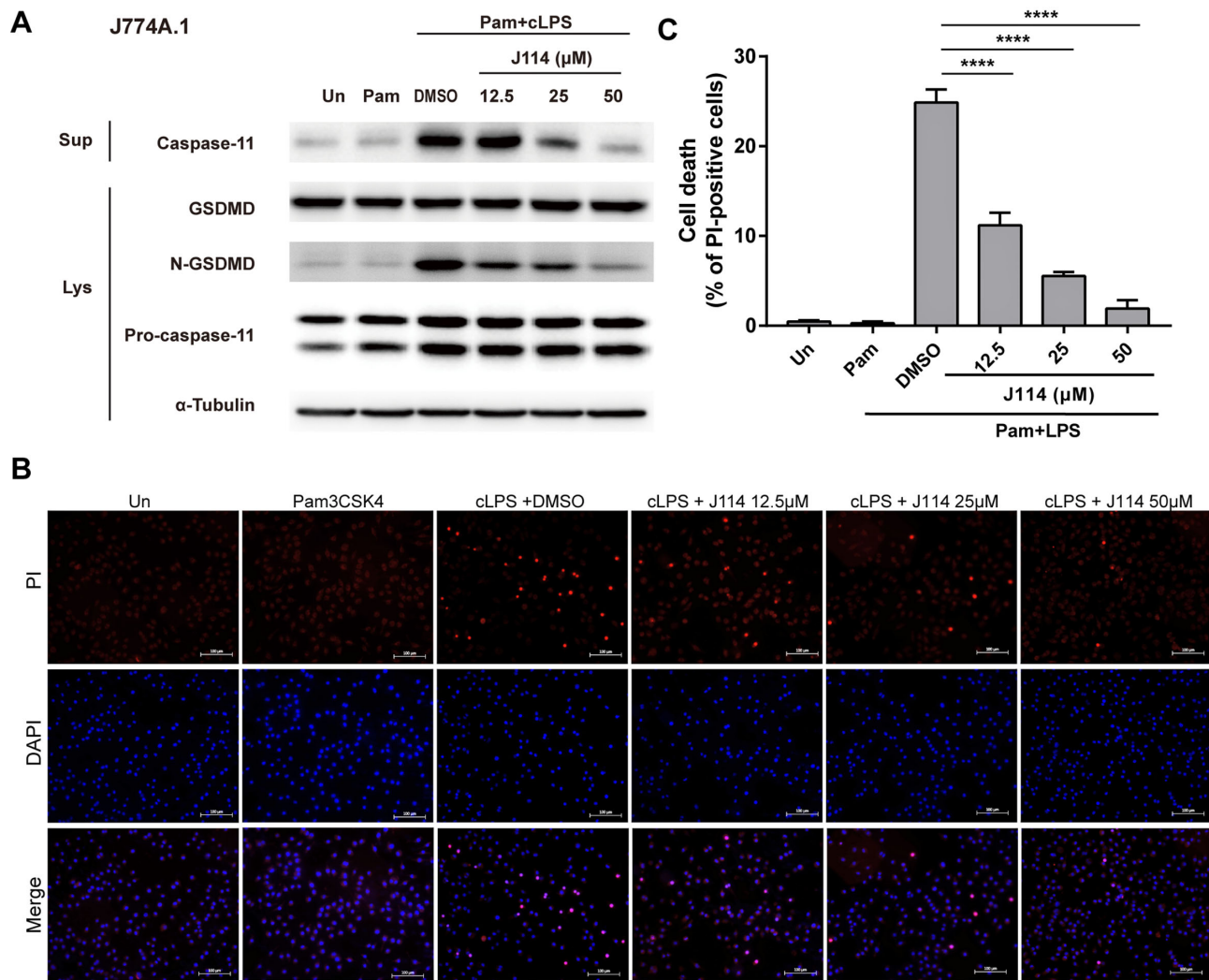


**FIGURE 2.** J114 inhibits caspase-11 activation and pyroptotic cell death in J774A.1 macrophages. Cells were primed with Pam3CSK4 (1 μg/mL) for 4 hours and then treated with the indicated doses of J114 for 30 minutes followed by transfection with 1 μg/mL lipopolysaccharide (LPS) overnight. (A) Lytic cell death fluorescent images showed PI-positive cells merged with DAPI. Scale bars, 100 μm. The result was representative of three independent experiments. (B) The percentage of PI-positive cells was quantified by counting six screenshots using ImageJ software. (C) Western blot analysis of protein levels in culture supernatants and cell lysates. The result was representative images of three independent experiments.

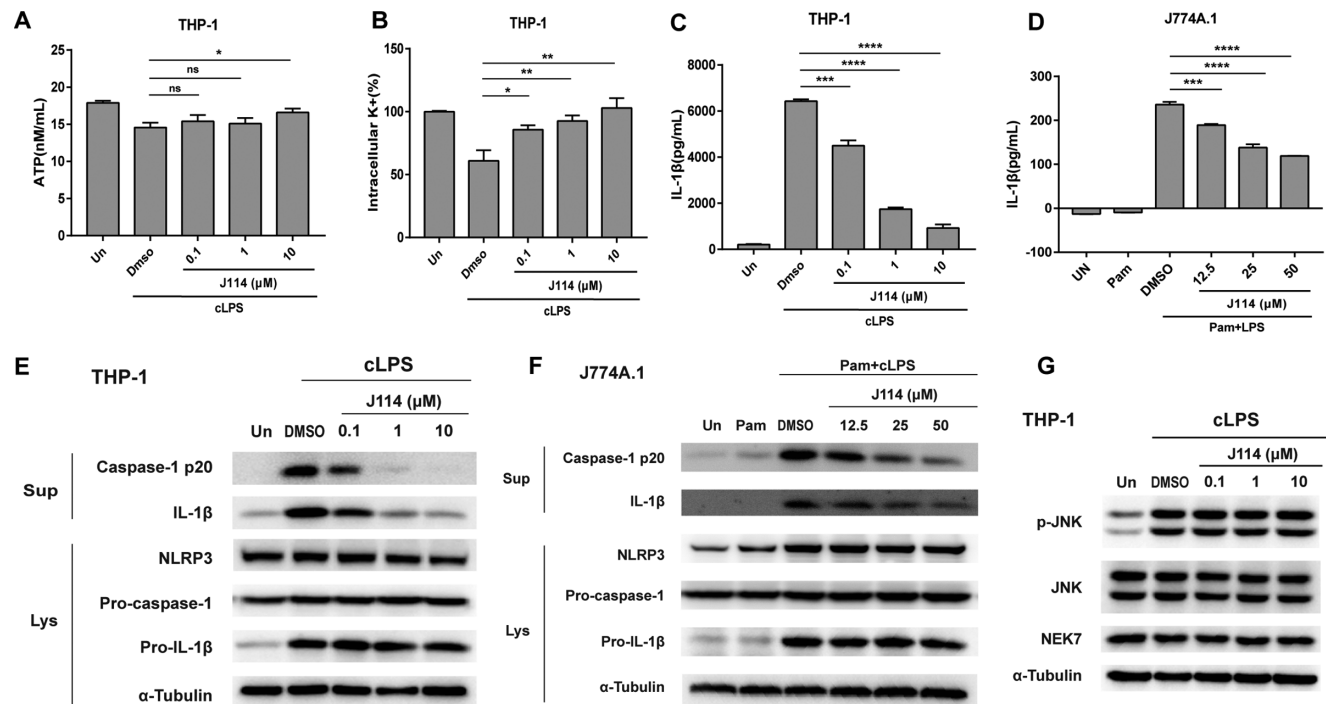


**FIGURE 3.** J114 inhibits the activation of the noncanonical NLRP3 inflammasome. (A) Cells were treated with the indicated doses of J114 for 30 minutes followed by transfection with 1 μg/mL lipopolysaccharide (LPS) overnight. Concentrations of intracellular ATP were determined by an Enhanced ATP Assay Kit ( $n = 3$ ). (B) Cells were treated as described previously, and the concentrations of intracellular K<sup>+</sup> were determined by potassium turbidimetry ( $n = 3$ ). (C) ELISA analysis of IL-1β in the supernatants of LPS-transfected THP-1 macrophages treated with the indicated dose of J114 ( $n = 3$ ). (D) J774A.1 cells were primed with 1 μg/mL Pam3CSK4 for 4 hours and treated with J114 at the indicated dose for 30 min, followed by transfection with 1 μg/mL LPS overnight. The production of IL-1β in the supernatants was measured by ELISA ( $n = 3$ ). The data are expressed as the mean ± SEM of three independent experiments A to D. (E) Western blot analysis of Sup and Lys from THP-1 macrophages treated with the indicated dose of J114 for 30 minutes before LPS transfection overnight. The results are representative images of three independent experiments. (F) Pam3CSK4-primed J774A.1 cells treated with J114 for 30 minutes before being transfected with LPS overnight. The supernatants (Sup) and cell lysates (Lys) were collected and analyzed by Western blotting. (G) Western blot analysis of p-JNK/JNK and NEK7 in the lysates from LPS-transfected THP-1 macrophages treated with the indicated doses of J114 for 30 minutes before. The result was representative images of three independent experiments E to G.

and then activates the NLRP3 inflammasome.<sup>14</sup> We next examined the effect of J114 on this process. First, we evaluated the effect of J114 on ATP release and K<sup>+</sup> efflux, which were upstream signaling events associated with noncanonical NLRP3 activation. Unexpectedly, the results showed that intracellular LPS stimulation induced the release of ATP and a dramatic decrease in intracellular potassium, and this effect could be partly reversed by J114 (Figs. 3A, 3B). Subsequently, immunoblot analysis showed that intracellular LPS induced the release of activated caspase-1 p20, further triggering the cleavage of pro-IL-1β and secretion of the activated form into the supernatants in both THP-1 and J774A.1 cells. Consistent with its inhibitory activity on caspase-4/5 and GSDMD activation, caspase-1 activation and IL-1β secretion triggered by transfected LPS were dose-dependently blocked by J114 in THP-1 and J774A.1 cells (Figs. 3C–F). Several kinases have been reported to be critical regulators of NLRP3 inflammasome activation, including the kinases JNK and NEK7.<sup>15</sup> Indeed, intracellular LPS stimulation significantly increased the phosphorylation of JNK and NEK7, which could not be inhibited by J114 (Fig. 3G). This suggested that J114 inhibited NLRP3 inflammasome activation independently of JNK or NEK7 phosphorylation. These results demonstrated that J114 specifically inhibited the caspase-4/5-dependent noncanonical pyroptosis pathway by reversing ATP release

and K<sup>+</sup> efflux and inhibiting noncanonical NLRP3 inflammasome activation.

### J114 Inhibits ASC Oligomerization

ASC speck formation is a hallmark of NLRP3 inflammasome activation. We next investigated whether J114 could inhibit the formation of ASC specks in noncanonical NLRP3 inflammasome activation. THP-1 ASC-GFP cells were transfected with LPS to induce the expression of GFP-fused ASC protein. As shown in Figures 4A, 4B, after intracellular LPS stimulation, a single ASC speck was observed in several cells, whereas the percentage of cells with an ASC speck was dose-dependently decreased after treatment with J114, which was consistent with the inhibitory effects on caspase-4/5 activation and IL-1β secretion. A similar result was observed in J774A.1 macrophage cells (Fig. 4C). To confirm the inhibition of ASC speck formation by J114, we performed an ASC oligomerization assay. The results showed that ASC dimers and oligomers were detected in the lysates of LPS-transfected THP-1 and J774A.1 macrophages. J114 significantly attenuated ASC oligomerization in a dose-dependent manner in both THP-1 and J774A.1 macrophages (Figs. 4D, 4E). However, the mechanism of the inhibitory effect of J114 on ASC oligomerization is still unknown. Next, we

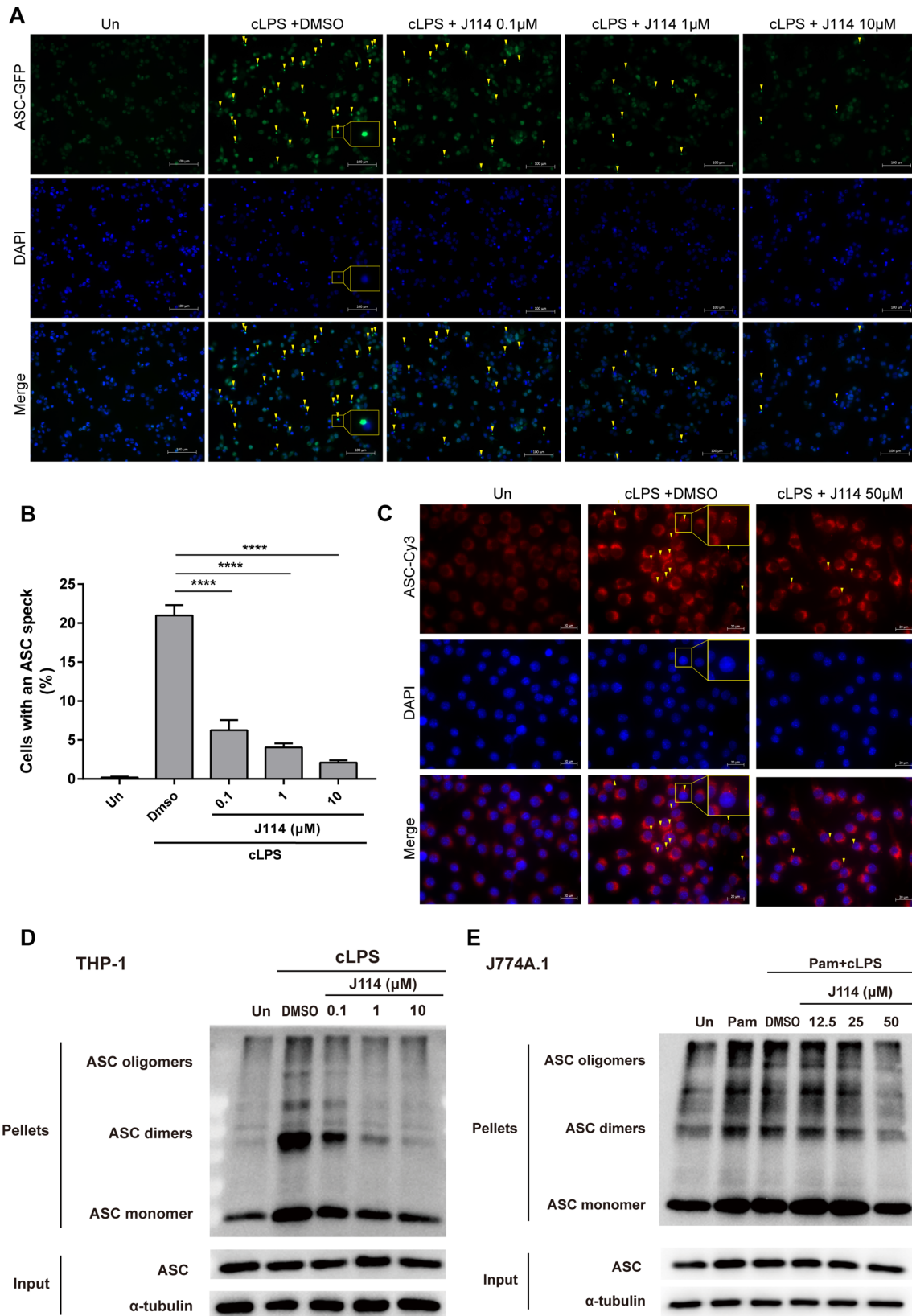


**FIGURE 4.** J114 inhibits apoptosis-associated speck-like protein containing CARD (ASC) oligomerization. (A) THP-1 ASC-GFP reporter cells were treated with different doses of J114 for 30 minutes and transfected with 1  $\mu$ g/mL LPS overnight. The cells were fixed with 4% paraformaldehyde and stained with DAPI. Immunofluorescence microscopy showed ASC specks (green) and nuclei (blue). Yellow arrowheads indicate ASC specks, and the partially enlarged inset shows one cell with an ASC speck. Scale bars, 100  $\mu$ m. The results are representative images of at least three independent experiments. (B) The percentage of ASC-GFP reporter cells containing an ASC speck was calculated



from 8 random fields using ImageJ software. Data are shown as the mean  $\pm$  SEM. (C) J774A.1 cells were primed with Pam3CSK4 for 4 hours and treated with J114 for 30 minutes, followed by transfection with 1  $\mu$ g/mL LPS overnight. Immunofluorescence microscopy shows ASC specks (red) and nuclei (blue). Yellow arrowheads indicate ASC specks, and the partially enlarged inset shows one cell with an ASC speck. Scale bars, 20  $\mu$ m. (D) Western blot analysis of crosslinked pellets and soluble lysates (Input) from THP-1 macrophages treated with the indicated doses of J114 for 30 minutes before being transfected with LPS overnight. The result was representative images of three independent experiments. (E) Western blot analysis of cross-linked pellets and soluble lysates (Input) from Pam3CSK4-primed J774A.1 cells treated with J114 for 30 minutes before being transfected with LPS overnight. The result was representative images of three independent experiments.

explored whether J114-mediated inhibition of noncanonical NLRP3 inflammasome activation is dependent on the NLRP3/ASC inflammasome pathway.

### J114-Mediated Inhibition of Noncanonical NLRP3 Inflammasome Activation is Dependent on the NLRP3 Inflammasome by Blocking the NLRP3-ASC Interaction

We then determined whether J114 is dependent on the NLRP3 inflammasome to inhibit noncanonical NLRP3 inflammasome activation. We performed experiments in THP-1 ASC-KO cells that lack ASC expression and are thus defective in the NLRP3/ASC pathway, resulting in no ASC, IL-1 $\beta$  or caspase-1 activation. The results showed that J114 could not inhibit either caspase-4/5 activation or N-GSDMD generation in THP-1 ASC-KO cells (Fig. 5A). Similar result was verified in RAM 264.7 murine macrophage cells that lack ASC expression (Fig. 5B). These results suggested that J114-mediated inhibition of noncanonical NLRP3 inflammasome activation was dependent on NLRP3 inflammasome assembly. Then, we explored whether J114 could impact the interaction of NLRP3 and ASC, which is a critical step for inflammasome assembly. Co-IF revealed that J114 blocked the NLRP3-ASC interaction in intracellular LPS-primed THP-1 macrophages (Figs. 5C–E). These results suggested that J114 inhibited noncanonical NLRP3 inflammasome assembly by blocking the NLRP3-ASC interaction.

### J114 Protected Against LPS-Induced Noncanonical Pyroptosis of Acute Keratitis in Mice

We finally verified whether J114 could inhibit noncanonical NLRP3 inflammasome activation and pyroptosis in vivo. Intrastromal injection of LPS was sufficient to trigger an obvious local inflammatory response in mouse corneas. The results showed corneal edema, opacity and swelling after LPS intervention, especially peaking at 48 hours (Figs. 6A, 6B). H&E staining was consistent with clinical features, which presented a destroyed and thickened corneal structure with extensive leukocytes infiltration (Fig. 6C). To explore whether the inflammatory cells, especially macrophage, infiltrated the corneal stromal layer during LPS-induced keratitis, single-cell suspensions of corneal tissues were examined with flow cytometry. CD45<sup>+</sup> leukocytes, CD45<sup>+</sup>CD11b<sup>+</sup>F4/80<sup>+</sup> macrophages, and CD86<sup>+</sup> proinflammatory (M1 phenotype) macrophages were increased dramatically in the corneas with LPS intrastromal injection (Figs. 6D, 6E). Meanwhile, double immunofluorescence staining revealed a strong colocalization of CD11b<sup>+</sup> with IL-1 $\beta$  and F4/80 with IL-1 $\beta$  in the corneas after LPS intrastromal injection (Figs. 6F, 6G). Similar result was observed in IHC staining for CD11b<sup>+</sup> and F4/80 (Figs. 6H, 6I). Therefore, macrophage infiltration is closely associated

with LPS-induced acute keratitis. These pathological features were obviously relieved in the J114-treated group, with alleviated corneal inflammation, milder opacity, less leukocytes infiltration, and less macrophages infiltration.

In addition, LPS intrastromal injection induced noncanonical pyroptosis in acute keratitis, and IHC staining for IL-1 $\beta$ , caspase-1, caspase-11, and NLRP3, showed activation of the inflammasome (Fig. 7A). Immunoblot analysis also confirmed the occurrence of noncanonical pyroptosis. J114 inhibited LPS-induced IL-1 $\beta$  secretion, caspase-1 and caspase-11 activation, and GSDMD cleavage (Figs. 7B, 7C), but did not injure the corneal epithelial layer (Supplementary Fig. S2). These results suggested that J114 alleviated corneal inflammation and protected against LPS-induced noncanonical pyroptosis in acute keratitis.

## DISCUSSION

Corneal inflammation caused by microbial infections is a major cause of corneal opacification and blindness worldwide.<sup>16</sup> Although microbes can be eliminated by antimicrobials, the activated immune system will not stop immediately, and the activated inflammatory state often lasts longer, causing more injury to the structure and function of the cornea.<sup>17</sup> During the innate immune response that occurs after corneal exposure to the pathogen, inflammasomes are known as the first responders to sense the presence of pathogens.<sup>18</sup> Subsequently, a cascade of events of pyroptosis is triggered, including the production of inflammatory factors following the activation of caspase, cell membrane pore formation following the cleavage of gasdermin-D, and eventual cell lysis with the release of more proinflammatory cytokines, which in turn causes inflammation to persist and relapse.<sup>5,19</sup> This is also the most difficult and challenging for keratitis treatment.

Previous studies have confirmed that LPS can induce acute keratitis through the noncanonical pyroptosis pathway.<sup>20,21</sup> The expression of caspase-4/5/11 and N-GSDMD in LPS-induced cell models, keratitis rat models, and patients with *P. aeruginosa* keratitis were all increased.<sup>22</sup> Thus, noncanonical pyroptosis is essential for the progression of corneal inflammation. Based upon the present study, we transfected LPS into cells to activate caspase-4/5/11, causing N-GSDMD-mediated pyroptosis and noncanonical NLRP3 inflammasome activation, which is a commonly used approach to induce a noncanonical pyroptosis model.<sup>23,24</sup> THP-1, J774A.1, and RAW264.7 cells, as macrophages patrolling various tissues in humans and mice, respectively, are critical innate immune cells for monitoring any microbial infections or tissue injury and can act as ideal model systems for preliminary investigation and selection of doses for in vivo studies.<sup>25,26</sup> Several studies have provided convincing evidence that lymphoid cells are a normal and noninflammatory component of the ocular surface.<sup>27</sup> Eye-associated lymphoid tissue maintains the physiological immune



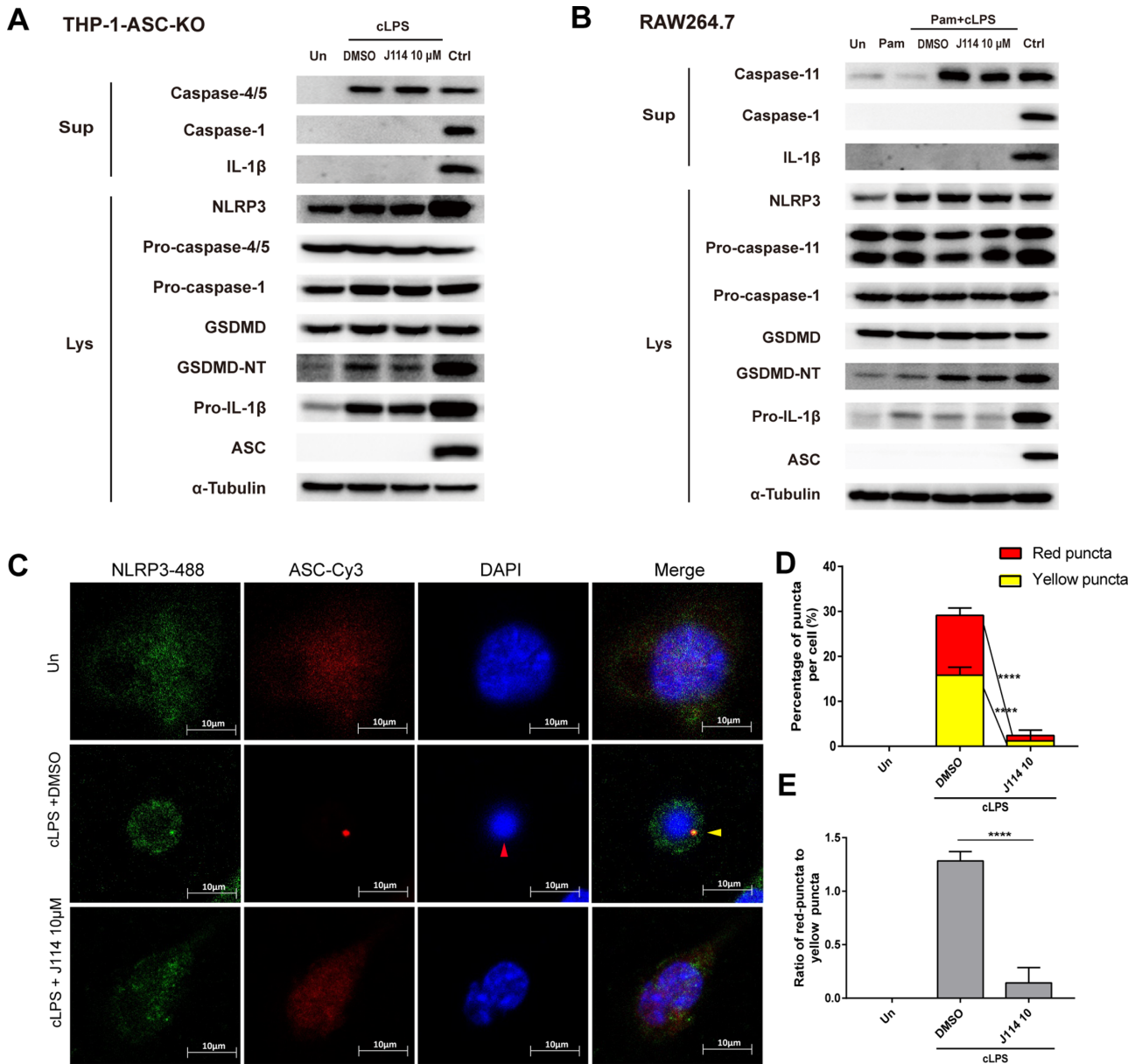


**FIGURE 5.** J114 inhibits the assembly of NLRP3 inflammasomes by blocking the NLRP3-ASC interaction. (A) THP-1 ASC-KO cells were treated with J114 and then transfected with 2.5  $\mu$ g/mL LPS overnight. Western blot analysis of the indicated proteins in culture supernatants (Sup) and cell lysates (Lys). Control (Ctrl) were the culture supernatant and cell lysate from THP-1 cells transfected with 1  $\mu$ g/mL LPS overnight. The result was representative images of three independent experiments. (B) RAW 264.7 cells (lacking ASC) were primed with Pam3CSK4 for 4 h and treated with J114 followed by transfection with 2.5  $\mu$ g/mL LPS overnight. Sup and Lys were collected and analyzed by Western blotting. Control (Ctrl) were the supernatants and lysates from J774A.1 cells transfected with 1  $\mu$ g/mL LPS overnight. The result was representative images of three independent experiments. (C) THP-1 cells were treated with J114 and then transfected with 1  $\mu$ g/mL LPS overnight. Confocal fluorescence microscopy was used to reveal the distribution of NLRP3 (green), ASC (red), and nuclei (blue). The representative image shows an ASC speck colocalized with the NLRP3 punctum, as revealed by a yellow dot in the merged image (yellow arrowheads). The cells transfected with LPS showed dying cells that lost cytoplasmic components with a shrunken nucleus (red arrowheads). Scale bar, 10  $\mu$ m. The result was representative images of three independent experiments. (D) The percentage of ASC speck and merged puncta was calculated from eight random fields using ImageJ software. (E) The ratio of ASC speck to merged puncta was calculated from eight random fields using ImageJ software. Data are shown as the mean  $\pm$  SEM.

protection of ocular surface, which is also believed to be crucial for the inflammatory pathogenesis.<sup>28</sup> Potential presentation of antigens of eye-associated lymphoid tissue would lead to recruit other immune cells and induce the inflammatory immune responses.<sup>27</sup> These immune cells in the target ocular tissues were shown to express specific markers, such as CD86<sup>+</sup>CD11b<sup>+</sup> macrophages, which could

produce proinflammatory cytokines and induce inflammation and tissue destruction.<sup>29</sup> In response to LPS stimulation, macrophages express inflammatory cytokines to activate more immune cells into infected tissue and induce pyroptotic cell death.<sup>30</sup> *in vivo*, LPS-induced corneal inflammation showed typical pathological features of keratitis, including corneal edema, opacity, and stromal infiltrates.<sup>12,20,31</sup>

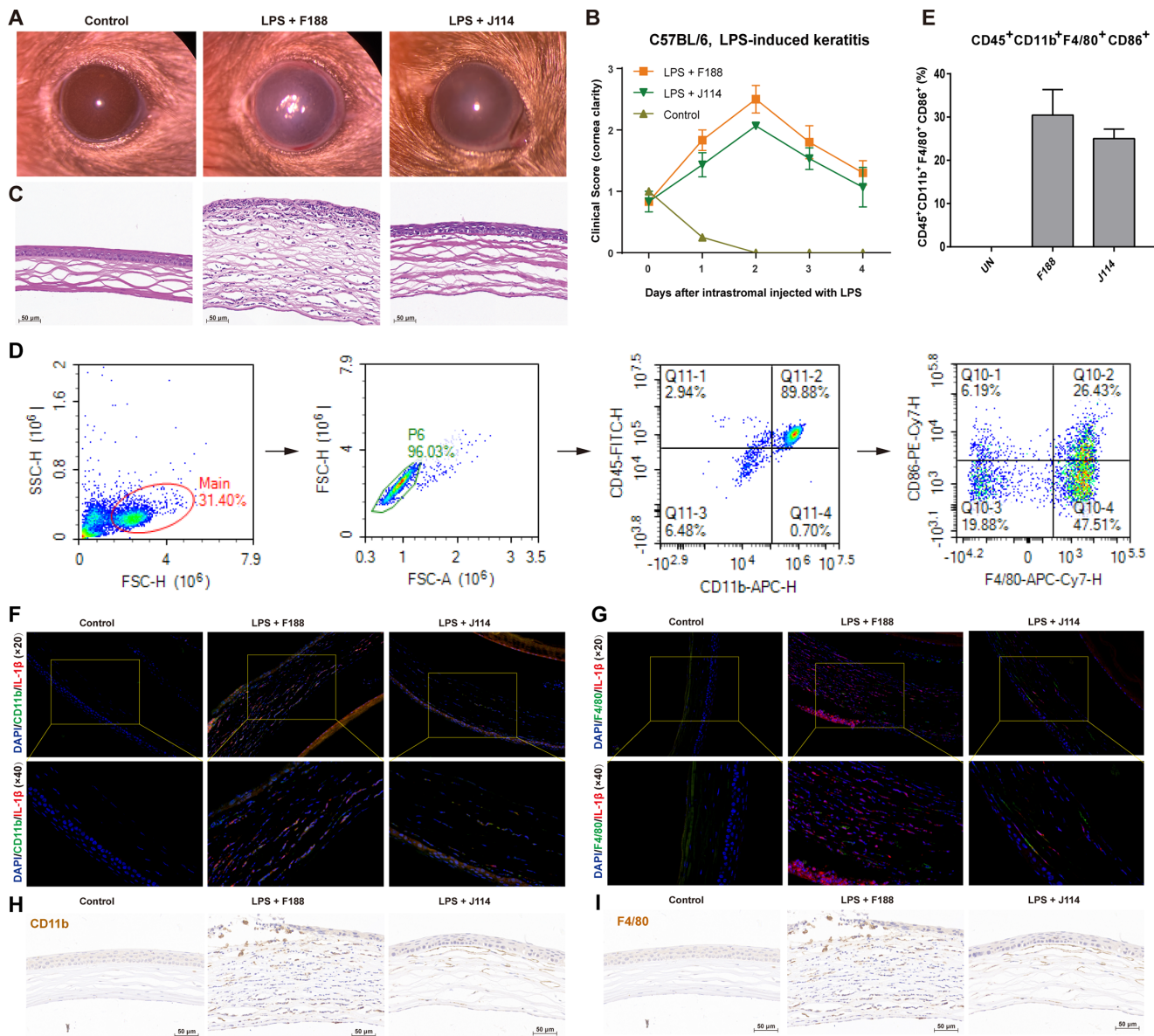


**FIGURE 6.** Macrophage infiltration in LPS-induced noncanonical pyroptosis of acute keratitis in mice. Mice were sham-operated or intrastromal injected with LPS (3  $\mu$ L 1 mg/mL) and treated with J114 or control four times a day. (A) Representative clinical images of LPS-induced acute keratitis in mouse corneas. (B) Mouse corneal clinical scoring was based on a 4-point system. Corneal edema, opacity, and swelling was most obvious 48 hours after LPS injection ( $n = 12$ ). (C) Representative histopathological examination (H&E staining) images of LPS-induced acute keratitis in mouse corneas. (D) Gating strategy for single cells, leukocytes, macrophages, and M1 phenotype macrophages. (E) The percentage of CD45<sup>+</sup>CD11b<sup>+</sup>F4/80<sup>+</sup>CD86<sup>+</sup> cells in corneal tissue at 48 hours after LPS injection ( $n = 12$ ). (F, G) Immunofluorescence staining displayed the colocalization of CD11b<sup>+</sup> with IL-1 $\beta$  and F4/80 with IL-1 $\beta$  in the corneas after LPS intrastromal injection. (H, I) Immunohistochemical analysis was performed to examine the expression of macrophage CD11b<sup>+</sup> and F4/80. These results were representative images of three independent experiments.

We previously screened and discovered a novel small molecular inhibitor against the NLRP3 inflammasome.<sup>11</sup> However, whether J114 inhibits noncanonical pyroptosis and attenuates corneal inflammatory reactions in vivo has not been determined. In the noncanonical pyroptosis process, caspase-4/5/11 are identified as the direct sensor of intracellular LPS and can be activated by identifying intracellular LPS.<sup>32</sup> Activated caspase-4/5/11 cleaves GSDMD to generate its N-terminal fragment, which executes pyroptosis by forming pores on the cell membrane.<sup>13,33</sup> Our results demonstrated that J114 potently inhibited caspase-4/5/11-dependent noncanonical pyroptosis in both human

and mouse macrophages and protected cells from pyroptotic death. In addition, activated caspase-4/5/11 induces ATP release and K<sup>+</sup> efflux to mediate the activation of the noncanonical NLRP3 inflammasome, leading to caspase-1 activation and IL-1 $\beta$  maturation.<sup>34,35</sup> Further biological studies revealed that J114 inhibited the activation of noncanonical NLRP3-dependent activation and release of IL-1 $\beta$  in macrophages through the effects of some upstream events, including ATP release and K<sup>+</sup> efflux, but had no effects on kinase phosphorylation. However, the accurate mechanism by which J114 acts upstream of NLRP3 inflammasome activation remains unknown.

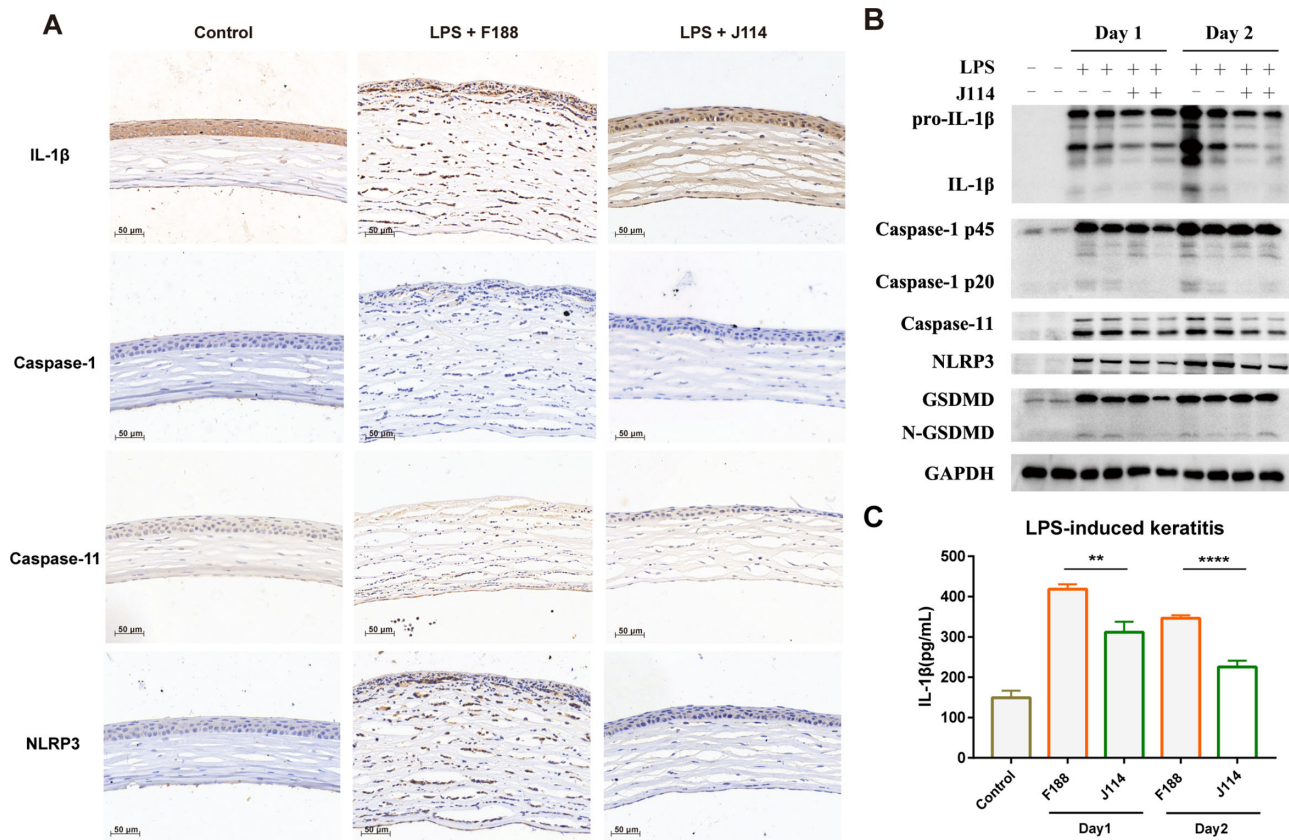


**FIGURE 7.** J114 protected against LPS-induced noncanonical pyroptosis of acute keratitis in mice. Mice were sham-operated or intrastromal injected with LPS (3  $\mu$ L 1 mg/mL) and treated with J114 or control four times a day. (A) Immunohistochemical analysis was performed to examine the expression of IL-1 $\beta$ , caspase-1, caspase-11, and NLRP3. (B) Lysates of mouse corneas were determined by Western blot 24 and 48 hours after LPS injection to show the expression of the indicated protein. The result was representative images of three independent experiments. (C) Intrastromal IL-1 $\beta$  level was determined by ELISA at 24 and 48 hours after LPS injection ( $n = 12$ ).

Further study is still needed to elucidate the underlying details.

The assembly of the NLRP3 inflammasome is a core of pyroptosis, which is a complex constructed by pattern recognition receptors NLRP3, apoptosis speck-like protein (ASC), and pro-caspase-1 and can activate caspase-1 to exert a proteolytic enzyme function.<sup>36,37</sup> This process is strictly dependent on ASC deficiency, which completely blocks inflammasome assembly.<sup>38</sup> Mechanistically, J114 potently suppressed ASC oligomerization but could not inhibit LPS-induced activation of caspase-4/5 in THP-1 ASC-KO and RAW264.7 cells lacking ASC expression. These results demonstrated that J114-mediated inhibition of noncanonical NLRP3 inflammasome activation is dependent on NLRP3/ASC. In fact, J114 reduced the interaction between NLRP3 and ASC, which might be the crucial role of J114 in potently inhibiting noncanonical pyroptosis and attenuating inflammation.

In vivo, previous studies have confirmed that LPS can induce acute corneal inflammation and cell injury by triggering the noncanonical pyroptosis signaling pathway.<sup>22</sup> Several drugs can attenuate inflammation in this process, such as resolvin D1, hepatocyte growth factor, and its derivative, N-palmitoyl-D-glucosamine and soluble Fas ligand.<sup>12,20,31,39–41</sup> However, all of these drugs mentioned above showed unsatisfactory activity and unclear targets. Our novel small molecular inhibitor J114 shows strong inhibitory activity at the

nM level and potently inhibits the NLRP3 inflammasome by reducing the interaction between NLRP3 and ASC. In vivo, J114 potently attenuated the inflammatory process and decreased stromal cell infiltration and corneal injury. Corneal damage is mediated by various cytokines, chemokines and their receptors produced by epithelial, stromal, and bone marrow-derived macrophages that contribute to cell damage and pyroptotic cell death.<sup>51,42</sup> Thus, J114 protected these cells from pyroptosis in LPS-induced keratitis with no sign of clinical irritation or damage.

In conclusion, our study demonstrated that a novel small molecular inhibitor, J114, prevents the progression of LPS-induced keratitis by inhibiting noncanonical pyroptosis and attenuating inflammatory cytokine release. Our data highlight the potent anti-inflammatory and pyroptosis protective functions of J114 both in vitro and in vivo. Therefore, J114 exhibits great potential as a promising and safe agent in the future in inflammatory ocular surface diseases.

### Acknowledgments

Supported by the China Postdoctoral Science Foundation (no. 2021M692273) and the Sichuan Provincial Science and Technology Support Project (no. 2022NSFSC1288, and no. 2022YFQ0070), and the National Natural Science Foundation of China (no. 82130104).



**Conflict of Interest:** The authors declare that the research was conducted in the absence of any commercial or financial relationships that could be construed as a potential conflict of interest.

Disclosure: **Y. Zhang**, None; **N. Zhou**, None; **Y. Jiao**, None; **G. Lin**, None; **X. Li**, None; **S. Gao**, None; **P. Zhou**, None; **J. Liu**, None; **J. Nan**, None; **M. Zhang**, None; **S. Yang**, None

## References

- Aragona P, Baudouin C, Benitez Del Castillo JM, et al. The ocular microbiome and microbiota and their effects on ocular surface pathophysiology and disorders. *Surv Ophthalmol*. 2021;66:907–925.
- Garcia-Vello P, Di Lorenzo F, Zucchetta D, Zamyatina A, De Castro C, Molinaro A. Lipopolysaccharide lipid A: A promising molecule for new immunity-based therapies and antibiotics. *Pharmacol Ther*. 2022;230:107970.
- Chen Y, Wang S, Alemi H, Dohlman T, Dana R. Immune regulation of the ocular surface. *Exp Eye Res*. 2022;218:109007.
- Man SM, Karki R, Kanneganti TD. Molecular mechanisms and functions of pyroptosis, inflammatory caspases and inflammasomes in infectious diseases. *Immunol Rev*. 2017;277:61–75.
- Swanson KV, Deng M, Ting JP. The NLRP3 inflammasome: molecular activation and regulation to therapeutics. *Nat Rev Immunol*. 2019;19:477–489.
- Chen M, Rong R, Xia X. Spotlight on pyroptosis: role in pathogenesis and therapeutic potential of ocular diseases. *J Neuroinflammation*. 2022;19:183.
- He Y, Hara H, Núñez G. Mechanism and Regulation of NLRP3 Inflammasome Activation. *Trends Biochem Sci*. 2016;41:1012–1021.
- Baker PJ, Boucher D, Bierschenk D, et al. NLRP3 inflammasome activation downstream of cytoplasmic LPS recognition by both caspase-4 and caspase-5. *Eur J Immunol*. 2015;45:2918–2926.
- Kayagaki N, Stowe IB, Lee BL, et al. Caspase-11 cleaves gasdermin D for non-canonical inflammasome signalling. *Nature*. 2015;526:666–671.
- Zhang X, Xu A, Lv J, et al. Development of small molecule inhibitors targeting NLRP3 inflammasome pathway for inflammatory diseases. *Eur J Med Chem*. 2020;185:111822.
- Jiao Y, Nan J, Mu B, et al. Discovery of a novel and potent inhibitor with differential species-specific effects against NLRP3 and AIM2 inflammasome-dependent pyroptosis. *Eur J Med Chem*. 2022;232:114194.
- Gregory-Ksander M, Perez VL, Marshak-Rothstein A, Ksander BR. Soluble Fas ligand blocks destructive corneal inflammation in mouse models of corneal epithelial debridement and LPS induced keratitis. *Exp Eye Res*. 2019;179:47–54.
- Kayagaki N, Warming S, Lamkanfi M, et al. Non-canonical inflammasome activation targets caspase-11. *Nature*. 2011;479:117–121.
- Zhang Y, Jiao Y, Li X, et al. Pyroptosis: A New Insight Into Eye Disease Therapy. *Front Pharmacol*. 2021;12:797110.
- Okada M, Matsuzawa A, Yoshimura A, Ichijo H. The lysosome rupture-activated TAK1-JNK pathway regulates NLRP3 inflammasome activation. *J Biol Chem*. 2014;289:32926–32936.
- Ung L, Bispo PJM, Shanbhag SS, Gilmore MS, Chodosh J. The persistent dilemma of microbial keratitis: Global burden, diagnosis, and antimicrobial resistance. *Surv Ophthalmol*. 2019;64:255–271.
- Singh RB, Das S, Chodosh J, et al. Paradox of complex diversity: Challenges in the diagnosis and management of bacterial keratitis. *Prog Retin Eye Res*. 2022;88:101028.
- Mathur A, Hayward JA, Man SM. Molecular mechanisms of inflammasome signaling. *J Leukoc Biol*. 2018;103:233–257.
- Shi J, Gao W, Shao F. Pyroptosis: Gasdermin-Mediated Programmed Necrotic Cell Death. *Trends in Biochem Sci*. 2017;42:245–254.
- Wang P, Zhu C, Liu M, Yuan Y, Ke B. The inhibiting effect of Aspirin Triggered-Resolvin D1 in non-canonical pyroptosis in rats with acute keratitis. *Exp Eye Res*. 2022;218:108938.
- Mandell JT, Vaccari JPR, Sabater AL, Galor A. The inflammasome pathway: A key player in ocular surface and anterior segment diseases [published online ahead of print July 4, 2022]. *Surv Ophthalmol*, <https://doi.org/10.1016/j.survophthal.2022.06.003>.
- Xu S, Liu X, Liu X, et al. Wedelolactone ameliorates *Pseudomonas aeruginosa*-induced inflammation and corneal injury by suppressing caspase-4/5/11/GSDMD-mediated non-canonical pyroptosis. *Exp Eye Res*. 2021;211:108750.
- Kayagaki N, Wong MT, Stowe IB, et al. Noncanonical inflammasome activation by intracellular LPS independent of TLR4. *Science*. 2013;341:1246–1249.
- Hagar JA, Powell DA, Aachoui Y, Ernst RK, Miao EA. Cytoplasmic LPS activates caspase-11: implications in TLR4-independent endotoxic shock. *Science*. 2013;341:1250–1253.
- Khatua S, Simal-Gandara J, Acharya K. Understanding immune-modulatory efficacy in vitro. *Chem Biol Interact*. 2022;352:109776.
- Chanput W, Mes JJ, Wichers HJ. THP-1 cell line: an in vitro cell model for immune modulation approach. *Int Immunopharmacol*. 2014;23:37–45.
- Knop E, Knop N. Influence of the eye-associated lymphoid tissue (EALT) on inflammatory ocular surface disease. *Ocul Surf*. 2005;3:S180–S186.
- Mastropasqua R, Agnifili L, Fasanella V, et al. The Conjunctiva-Associated Lymphoid Tissue in Chronic Ocular Surface Diseases. *Microsc Microanal*. 2017;23:697–707.
- Murray PJ, Allen JE, Biswas SK, et al. Macrophage activation and polarization: nomenclature and experimental guidelines. *Immunity*. 2014;41:14–20.
- Andersson U. Hyperinflammation: On the pathogenesis and treatment of macrophage activation syndrome. *Acta Paediatr*. 2021;110:2717–2722.
- Petrillo F, Trotta MC, Bucolo C, et al. Resolvin D1 attenuates the inflammatory process in mouse model of LPS-induced keratitis. *J Cell Mol Med*. 2020;24:12298–12307.
- Shi J, Zhao Y, Wang Y, et al. Inflammatory caspases are innate immune receptors for intracellular LPS. *Nature*. 2014;514:187–192.
- Liu X, Zhang Z, Ruan J, et al. Inflammasome-activated gasdermin D causes pyroptosis by forming membrane pores. *Nature*. 2016;535:153–158.
- He WT, Wan H, Hu L, et al. Gasdermin D is an executor of pyroptosis and required for interleukin-1 $\beta$  secretion. *Cell Res*. 2015;25:1285–1298.
- Rühl S, Broz P. Caspase-11 activates a canonical NLRP3 inflammasome by promoting K(+) efflux. *Eur J Immunol*. 2015;45:2927–2936.
- Martinon F, Burns K, Tschopp J. The inflammasome: a molecular platform triggering activation of inflammatory caspases and processing of proIL-beta. *Mol Cell*. 2002;10:417–426.
- Lamkanfi M, Declercq W, Kalai M, Saelens X, Vandenaabeele P. Alice in caspase land. A phylogenetic analysis of caspases from worm to man. *Cell Death Differ*. 2002;9:358–361.



38. Sharma M, de Alba E. Structure, Activation and Regulation of NLRP3 and AIM2 Inflammasomes. *Int J Mol Sci.* 2021;22:872.
39. Elbasiony E, Cho W, Mittal SK, Chauhan SK. Suppression of lipopolysaccharide-induced corneal opacity by hepatocyte growth factor. *Sci Rep.* 2022;12:494.
40. Iannotta M, Belardo C, Trotta MC, et al. N-palmitoyl-D-glucosamine, a Natural Monosaccharide-Based Glycolipid, Inhibits TLR4 and Prevents LPS-Induced Inflammation and Neuropathic Pain in Mice. *Int J Mol Sci.* 2021;22:1491.
41. Zhu S, Xu X, Wang L, et al. Inhibitory effect of a novel peptide, H-RN, on keratitis induced by LPS or poly(I:C) in vitro and in vivo via suppressing NF- $\kappa$ B and MAPK activation. *J Transl Med.* 2017;15:20.
42. Torricelli AA, Santhanam A, Wu J, Singh V, Wilson SE. The corneal fibrosis response to epithelial-stromal injury. *Exp Eye Res.* 2016;142:110–118.